HiSOR

ACTIVITY REPORT

2016

Hiroshima Synchrotron Radiation Center, HiSOR
Hiroshima University

HiSOR
ACTIVITY REPORT

2016

Hiroshima Synchrotron Radiation Center, HiSOR

Hiroshima University

Edited by Y. Izumi

The annual report is available from

Hiroshima Synchrotron Radiation Center, Hiroshima University
Kagamiyama 2-313, Higashi-Hiroshima 739-0046, JAPAN

Phone: +81-82-424-6293
Fax: +81-82-424-6294
e-mail: hisor@hiroshima-u.ac.jp
URL: http://www.hsrc.hiroshima-u.ac.jp/

Preface

The Hiroshima Synchrotron Radiation Center is the only one synchrotron radiation facility attached to a national university in Japan. It was established in 1996, as part of the academic policies of the Japanese government. A compact 700MeV electron-storage ring, HiSOR, produces synchrotron radiation in the ultraviolet and soft x-ray range. The mission of the center is to promote advanced research in the field of condensed matter physics using synchrotron radiation, as well as to develop human resources. In 2010, the center was authorized as a “Joint Usage / Research Center” by the Ministry of Education, Culture, Sports, Science and Technology (MEXT). As a result of extensive research activities in collaboration with researchers from inside and outside of Japan, the center was graded “A” in the term-end evaluation in 2015. In 2016, the authorization as the Joint Usage / Research Center was extended for next 6 years.

From fiscal year 2016 (FY2016) onwards, we improved our beamtime application procedure; we now call for proposals twice a year (Period A: April - October, Period B: November - March) to timely meet beamtime requests. At the same time, we reserve part of the available beamtime for urgent proposals of high scientific impact. In FY2016, 240 researchers including undergraduate and graduate students conducted 120 proposals. About 20% of the researchers are from abroad. You will find more detailed status and scientific activities of the center in this Activity Report 2016.

This fiscal year, three new staff members joined our center. Dr. Keigo Kawase (Associate Professor) and Dr. Shunya Matsuba (Assistant Professor) will lead the Accelerator Physics Laboratory. Dr. Yudai Izumi (Assistant Professor), an expert in radiation biology, will explore the interdisciplinary research field between condensed matter physics and life science, in collaboration with Dr. Koichi Matsuo (Associate Professor, promoted in FY2016).

A micro-spot high-resolution angle-resolved photoemission spectroscopy (μ-ARPES) machine using an ultraviolet (UV) laser has been successfully commissioned in our R&D laboratory. By using a focused UV laser beam (ϕ<5μm) and a specially developed high-precision sample manipulation system, high spatial, momentum and energy resolutions could be achieved at the same time. Since FY2016 collaborators from Japan and abroad have taken advantage of this powerful combination and investigated spatial variation of fine electronic structures of strongly correlated rare-earth compounds, high-Tc superconductors, and

topological materials. This project was initiated by the recommendation of the Advisory Committee of the center as a firm step towards our future scientific and technical challenges to utilize highly brilliant synchrotron radiation. Accumulated key technologies, such as precise manipulation and monitoring of samples, and newly developed software for quick spatial and precise angular mapping, will be utilized to the full extent in our future beamlines on the upgraded storage ring “HiSOR II”.

In closing, I would like to thank all of the staff members for their efforts to operate HiSOR, and to maintain and advance experimental stations. I would also like to thank our students and collaborators for their excellent scientific achievements, making full use of the facilities. Finally, I deeply appreciate the continued supports by Hiroshima University and MEXT.

July 2017

Kenya Shimada

Kenya Shimada
Director of Hiroshima Synchrotron Radiation Center

Table of Contents

— Off-line Experiments —

Appendices

Current Status of HiSOR

Status of the HiSOR storage ring

1. Introduction

The HiSOR is a synchrotron radiation (SR) source of Hiroshima Synchrotron Radiation Center, Hiroshima University, established in 1996. It is a compact racetrack-type storage ring having 21.95 m circumference, and its natural emittance of 400π nmrad is rather large compared with those of the other medium to large storage rings. The most outstanding advantage of the facility lies in good combination with state-of-the-art beamlines (BL's) for high-resolution photoelectron spectroscopy in the photon energy ranges between VUV and soft X-ray. The principal parameters of HiSOR are shown in Table 1.

Table 1: Main parameters of the HiSOR Storage ring.

Circumference	21.95 m
Type	Racetrack
Bending radius	0.87 m
Beam energy at Injection	150 MeV
at Storage	700 MeV
Magnetic field at Injection	0.6 T
at Storage	2.7 T
Injector	150 MeV Racetrack Microtron
Betatron tune (ν_x, ν_y)	(1.72, 1.84)
RF frequency	191.244 MHz
Harmonic number	14
RF voltage	200 kV
Stored current (nominal)	350 mA
Natural emittance	400π nmrad
Beam life time	~10 hours@200 mA
Critical wavelength	1.42 nm
Photon intensity (5 keV)	1.2×10^{11} /sec/mr^2/0.1%b.w./300mA

The originally designed maximum stored current of HiSOR was 300 mA. However, after the improvement of the control system and the RF system in 2003, HiSOR has been in operation with 350 mA maximum stored current since. Fig. 1 shows an example of typical one-day operation. Beam injection for HiSOR is executed twice a day, at around 9:00 and 14:30.

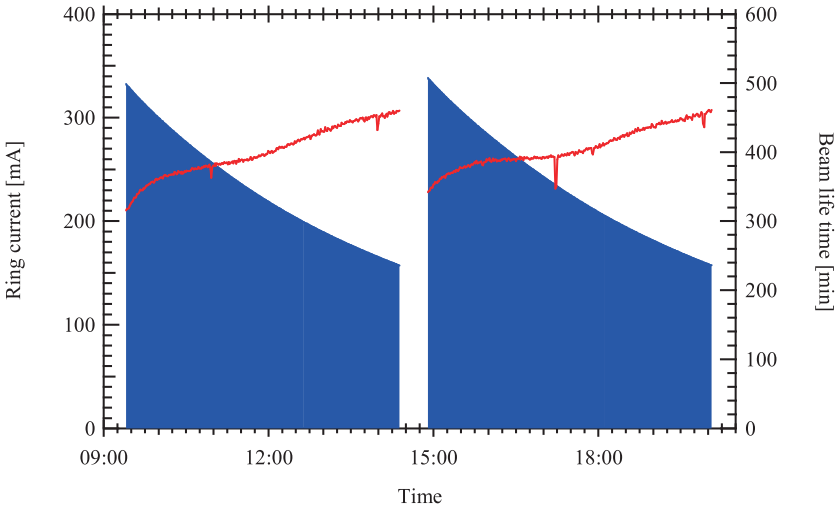

Fig. 1: Typical daily operation status.

HiSOR has two 180-deg. Normal-conducting bending magnets which generate a strong magnetic field of 2.7 T. This storage ring is equipped with two insertion devices, a linear undulator and a quasi-periodic APPLE-II undulator which replaced to the previous helical undulator in summer 2012. Major parameters of these undulators are listed in Table 2. The photon energy spectra of the SR from HiSOR are shown in Fig. 2.

Table 2: Main parameters of the undulators.

Linear undulator (BL-1)	
Total length	2354.2 mm
Periodic length λu	57 mm
Periodic number	41
Pole gap	30-200 mm
Maximum magnetic field	0.41 T
Magnetic material	Nd-Fe-B (NEOMAX-44H)
Quasi-Periodic APPLE-II undulator (BL-9A,B)	
Total length	1845 mm
Periodic length λu	78 mm
Periodic number	23
Pole gap	23-200 mm
Maximum magnetic field	0.86 T (horizontal linear mode)
	0.59 T (vertical linear mode)
	0.50 T (helical mode)
Magnetic material	Nd-Fe-B (NEOMAX-46H)

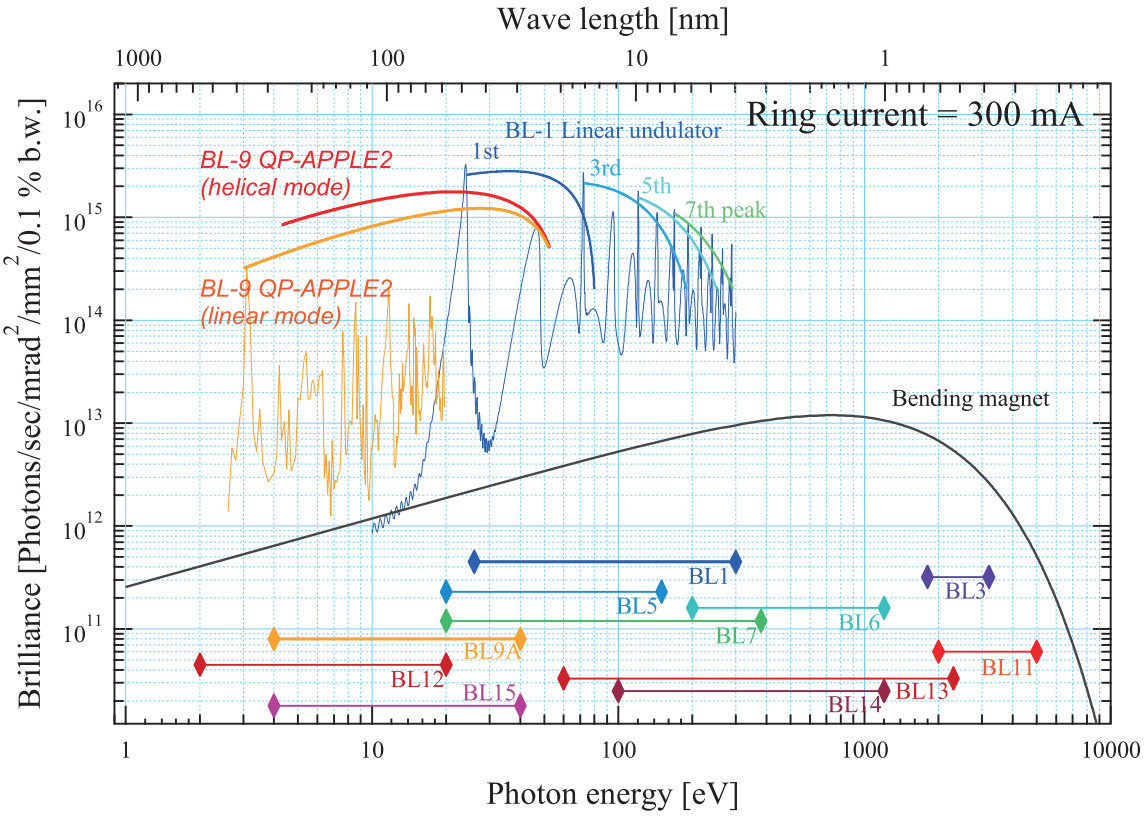

Fig. 2: Photon energy spectra of the SR from HiSOR.

2. Operation status in FY 2016

Fig. 3 shows monthly operation time of HiSOR storage ring in FY 2016. HiSOR has a long term cease period to have routine inspections in summer every year. The total user time of FY2016 achieved 1564 hours. Fig. 4 shows bar graph of total operation days in each fiscal year. It shows that days for user run in FY2016 was recovered those before occurring the trouble on vacuum (see “HiSOR Activity Report 2014” in detail). Operation times of the storage ring and the Microtron from FY 2007 to FY 2016 are shown in Fig. 5.

Most remarkable thing in the maintenance of the storage ring is that we have started to replace the microwave amplifier for the accelerating cavity from that using vacuum tubes to solid-state one. Comparing with the vacuum tube, in general, the solid-state amplifier has a good stability and reproducibility for a long term operation and it has a high cost performance for the maintenance because it consists of bundling small amplifier modules, thus, we will achieve more reliable operation for the storage ring in near future. The commissioning of the solid-state amplifier will be finished in early 2017 and it will be used in normal operation without any interruption.

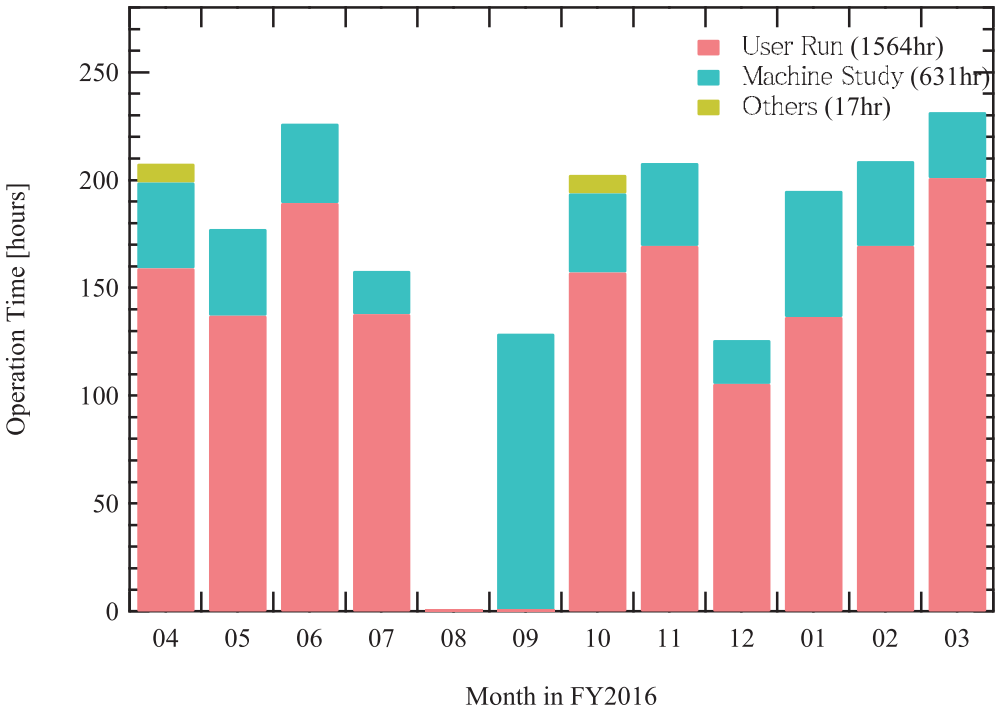

Fig. 3: Monthly operation time in FY 2016.

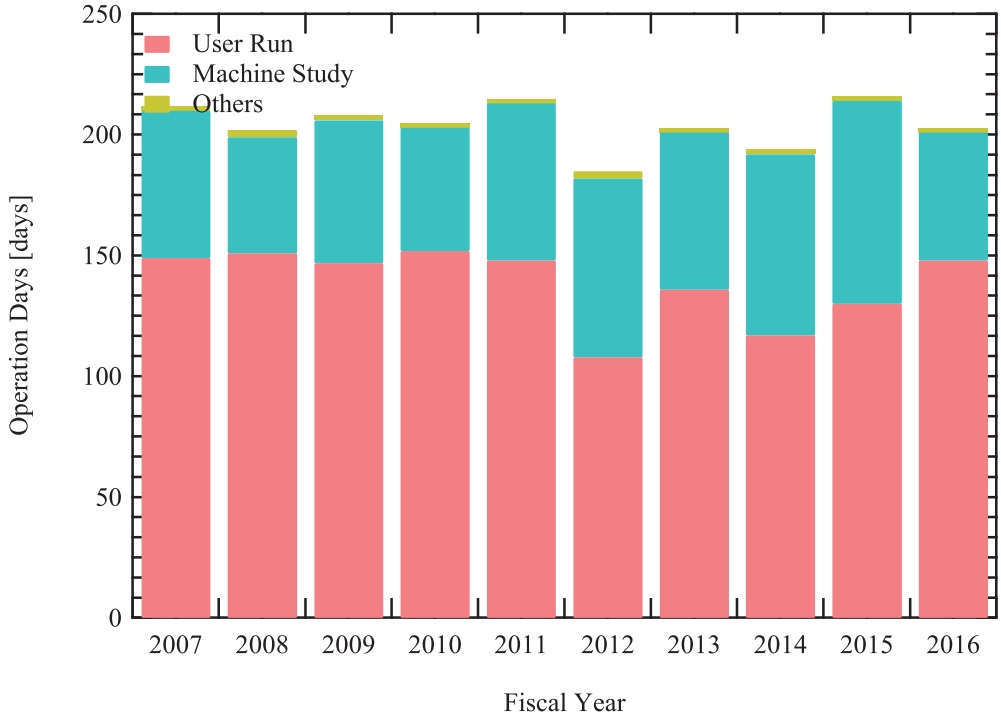

Fig. 4: Operation days of HiSOR storage ring.

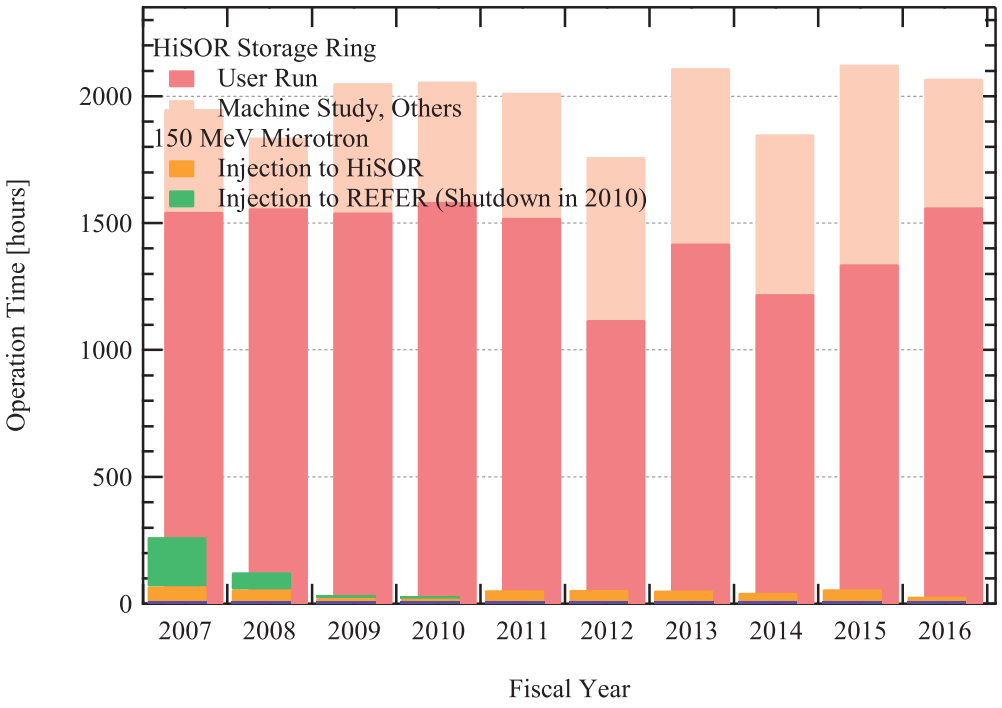

Fig. 5: Annual operation time of Storage ring and Microtron.

Beamlines

A total of 13 beamlines has been constructed so far; three normal-incidence monochromators, seven grazing-incidence monochromators, two double crystal monochromators and apparatus for white beam irradiation (Fig. 1). Table 1 lists the beamlines at present together with the main subject, energy range and monochromators.

Table 1: List of Beamlines

Beamline	Source	Monochromator	Subject	Energy range (eV)	Status
BL-1	LU	GIM	Polarization dependent high-resolution ARPES	22-300	In use
BL-3	BM	DCM	Surface XAFS	1800-3200	In use
BL-4	BM		White beam irradiation		Closed
BL-5	BM	GIM	ARPES and PEEM	40-220	In use
BL-6	BM	GIM	Gas-phase photochemistry	200-1200	In use
BL-7	BM	GIM	ARPES	20-380	In use
BL-8	BM		Beam diagnosis		In use
BL-9A	HU/LU	NIM		5-35	In use
BL-9B	HU/LU	GIM	High-resolution spin-resolved ARPES	16-300	In use
BL-11	BM	DCM	XAFS	2000-5000	In use
BL-12	BM	NIM	VUV-CD of biomaterials	2-10	In use
BL-13	BM	GIM	Surface photochemistry	60-1200	In use
BL-14	BM	GIM	Soft-XMCD of nano-materials	400-1200	In use
BL-15	BM	NIM	VUV-CD of biomaterials	4-40	Closed
BL-16	BM		Beam profile monitor		In use

At present, nine beamlines BL1, BL3, BL6, B7, BL9A, BL9B, BL11, BL12, BL13 and BL14 are opened for users. Furthermore, three offline systems, resonant inverse photoemission spectrometer (RIPES), low-temperature scanning tunneling microscope (LT-STM) system, high-resolution angle-resolved photoemission spectrometer using ultraviolet laser (Laser ARPES) are in operation (Fig. 2).

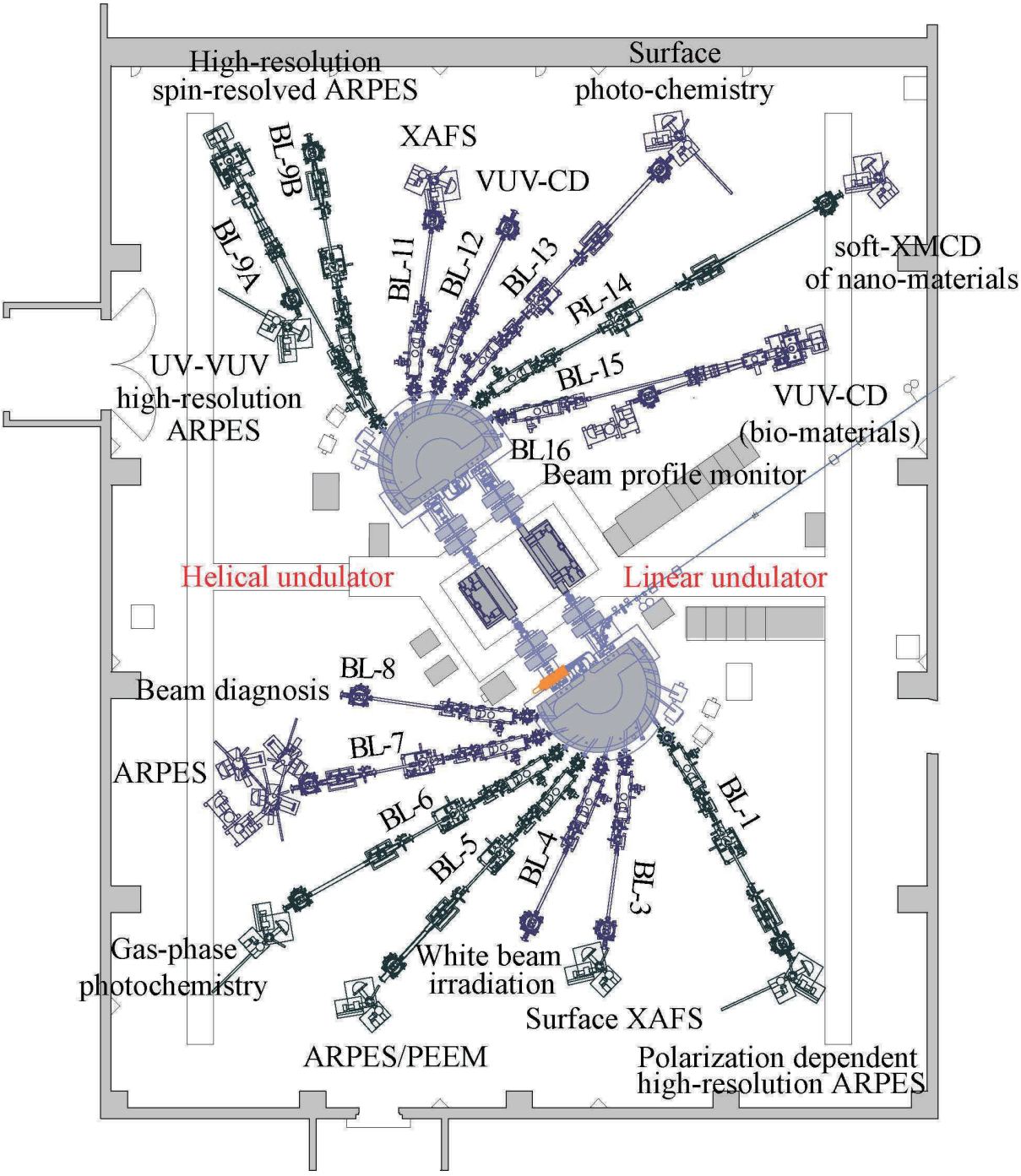

Fig. 1: Schematic view of the experimental hall.

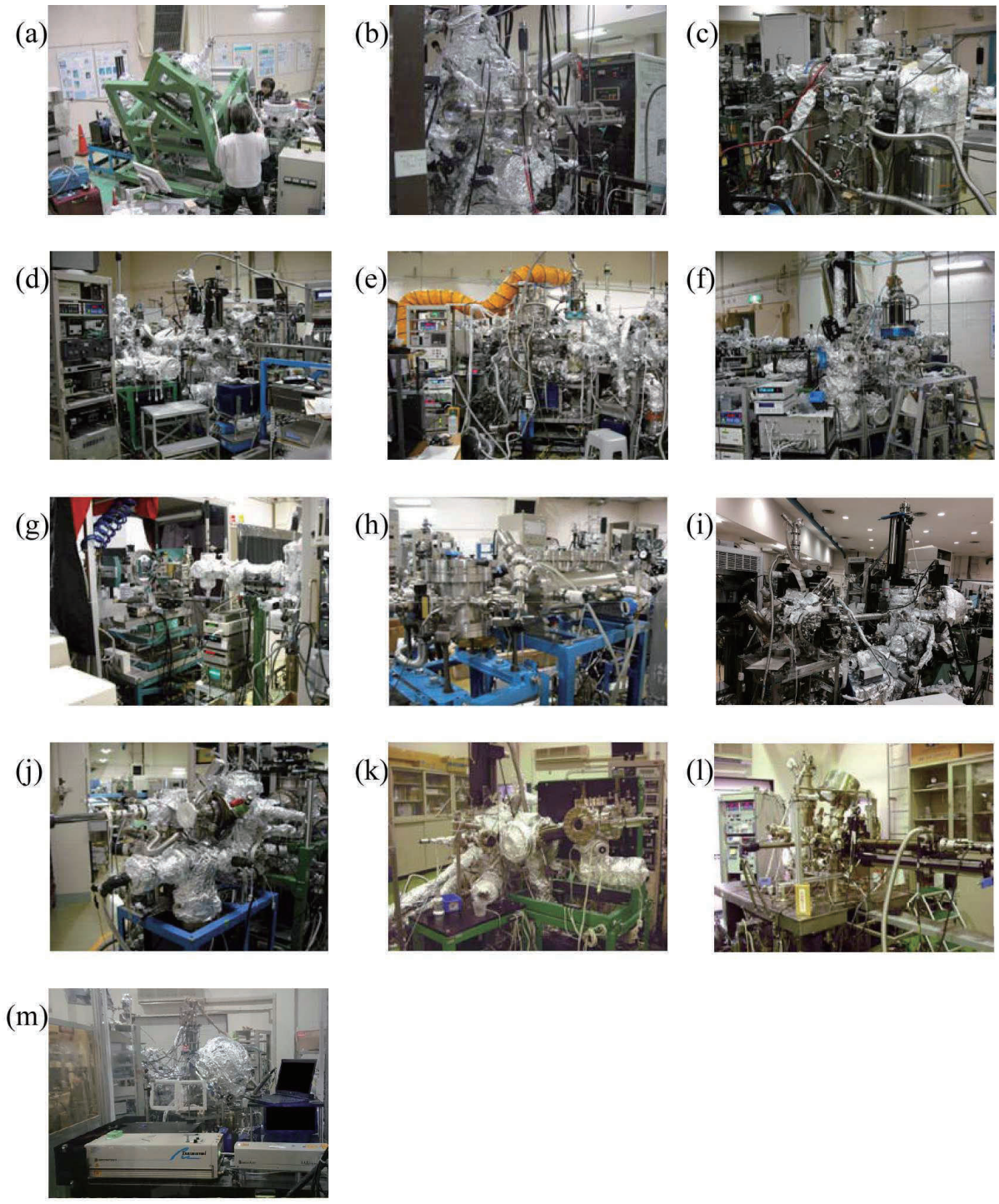

Fig. 2: Experimental stations on the beamline and offline: (a) BL-1, (b) BL-3, (c) BL-6, (d) BL-7, (e) BL-9A, (f) BL-9B, (g) BL-11, (h) BL-12, (i) BL-13, (j) BL-14, (k) RIPES (offline), (l) LT-STM (offline), (m) Laser ARPES (offline).

Research Activities

– Accelerator Studies –

Interference Experiment of Synchrotron Radiation from Two APPLE-Ⅱ Type Undulators at UVSOR-Ⅲ

Jin Kimura[a] and Shunya Matsuba[b]

[a]*Department of Physical Science, Faculty of Science, Hiroshima University*
1-3-1 Kagamiyama, Higashi-Hiroshima, 739-8526, Japan
[b]*Hiroshima Synchrotron Radiation Center, Hiroshima University*
2-313 Kagamiyama, Higashi-Hiroshima, 739-0046, Japan

Keywords: spiral interference pattern, undulator radiation

We carried out an interference experiment of synchrotron radiation from two APPLE-Ⅱ type undulators at the 3rd generation electron storage ring UVSOR-Ⅲ. The fundamental radiation was superimposed with the 2nd harmonic radiation and we observed interference patterns. In these patterns, it had been considered that states of linear polarization in patterns that looks spiral image were changed in rotating a linear polarizer, however, detail analysis had not been done. Therefore, we analyzed the intensity distribution of spiral patterns and visualized the directions of linear polarization plotting arrows (shown in **FIGURE 1**). Analyzing these polarization we also discussed spiral rotation associated with optical path difference.

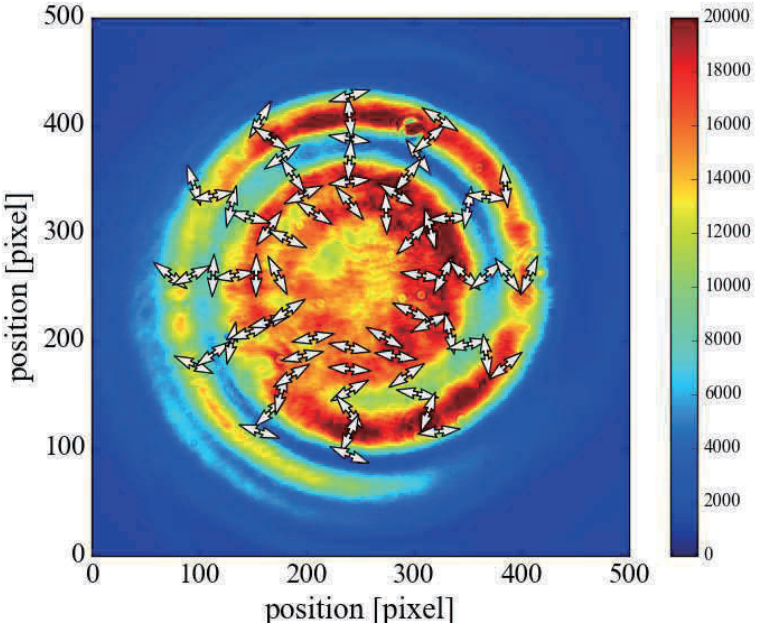

FIGURE 1. The distribution of linear polarization directions in the spiral interference pattern.

Research for the spectrum of the quasi-periodic undulator radiation to have a different quai-periodicity

Hatsuya Mima[a] Toshiya Matsuba[b] and Keigo Kawase[b]

[a] *Department of Physical Science, Graduate school of science, Hiroshima University*

[b]*Hiroshima Synchrotron Radiation Center, Hiroshima University*

The synchrotron radiation spectrum generated by a periodic linear undulator contains higher harmonics of integral multiple of fundamental harmonic in the spectrum. These higher harmonics are usually an obstacle to user's experiments. Therefore, to reduce higher harmonic contamination, such a user has to use many optical elements such as monochromator, band-pass filter, mirror to eliminate unwanted harmonics. However, such kind of beamline setup from an undulator to an end-station may cause a reduction of photon beam intensity. In order to ease such difficulties, quasi periodic undulator was developed in which higher harmonics appear at irrational positions instead of rational positions in the spectrum. A combination of a quasi-periodic undulator (QPU) and a single monochromator can provide purely monochromatic photon beam for end-users.

Until today, quasi periodic undulators used in all over the world are designed such that the peak magnetic field strength at certain positions representing the quasi-periodicity is reduced to introduce a smaller phase advance of photon wave at every QP position in an undulator. In this study, I aimed to obtain from a different quasi-periodicity for end-users. Fig.1 shows to way to make a quasi-periodicity. Fig.2 shows spectra to obtain from a different quasi-periodicity

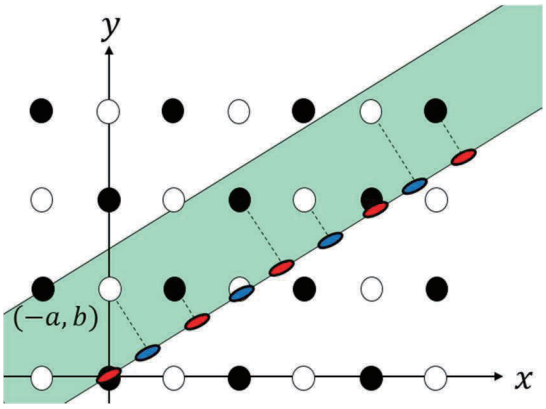

Fig.1. The way to make a quasi-periodicity

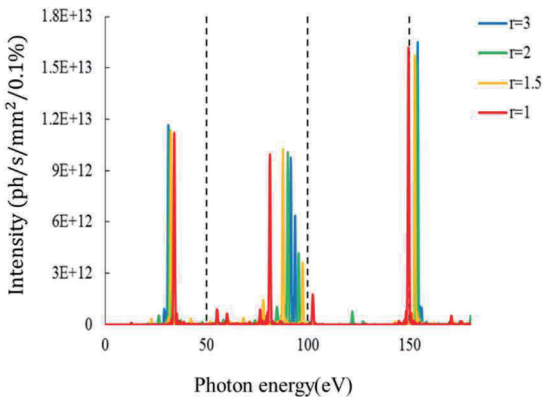

Fig.2. Radiation spectrum from magnetic field to have a different quasi-periodicity

REFERENCES

[1] S. Hashimoto and S. Sasaki, Nucl. Instr. Methods in Phys. Res. **A361**, 611, (1995).

[2] S. Sasaki, et.al, Proceedings of EPAC'98, p.2237, Stockholm, Sweden, 1998.

[3] S. Sasaki, Proceedings of IPAC'10. p.3141, Kyoto, Japan, 2010.

Simulation Study for improving the injection efficiency at KEK-PF

Kota Hirano[a] , Keigo Kawase[b] and Syunya Matsuba[b]

[a]*Department of Physical Science, Faculty of Science, Hiroshima University*
[b]*Hiroshima Synchrotron Radiation Center, Hiroshima University*

Keywords: electron storage ring, tracking simulation

In recent years, reduction of injection efficiency has become a problem in KEK-PF. It is thought the injection parameters have changed by increasing errors on the alignment of accelerator components due to the influence of the earthquake on March 11, 2011. However, the obvious cause is not known. It is desired to solve problems because the injection efficiency of kicker injection has decreased, it is not possible to enter the experimental station during accumulation of sored beam current. Normally, the incident beam is directed at the optimum angle by the septum electromagnet. At the same time, bumps are made against the central trajectory of the stored beam only moment of injection to suppress the initial amplitude of the betatron oscillation. Later it intersects the central orbit by the radiation dumping.

Such incidence simulation is possible with the simulator code SAD (Strategic Accelerator Design) for accelerator design developed by KEK. In the past, SAD has been used by development of multipole electromagnets injection system of KEK-PF. Therefore, we study the cause of beam loss by simulation of KEK-PF using SAD.

The injection beam consisting of gaussian distributed particles in the 6 dimensional phase space was prepared. The injection beam was made using the Twiss parameter, at the exit of the septum magnet, the emittance of the incident beam, the beam spread, etc. The initial position and incidence angle of the septum magnet were set to 27 mm and 2 mrad. When we simulate particle tracking using this injection beam, and it was found that particles were lost at several tens of turns. For this reason, we define capture efficiency as 100 turns and examine the change of capture efficiency in the vertical and horizontal direction. From this result the capture efficiency is improved as the position closer to the septum wall in the horizontal direction. The capture efficiency is improved when the amplitude of the beam is suppressed in the vertical direction. As a future prospect, we will find the beam loss position by placing an aperture at a place that physically limits the incident beam.

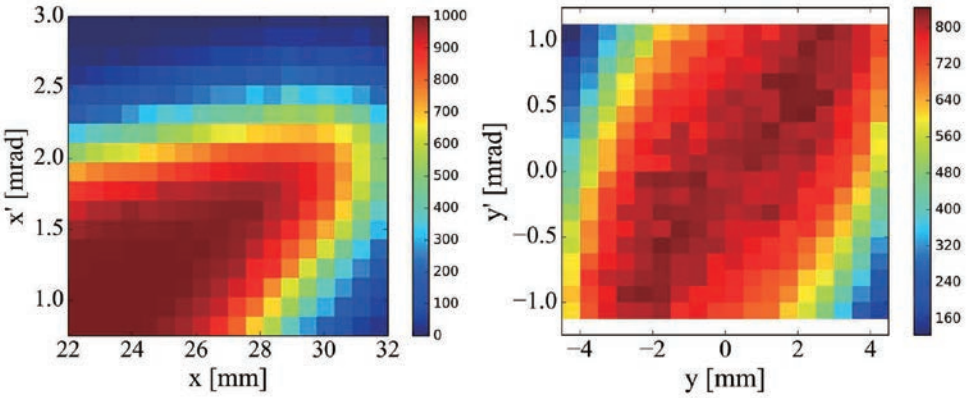

FIGURE1. change in capture efficiency in horizontal and vertical direction

REFERENCES

1. Hiroyuki Takagi: New injection scheme using a pulsed quadrupole magnet in the electron storage rings, The Graduate University for Advanced Studies, (2010)
2. SAD Home Page: http://acc-physics.kek.jp/SAD/K. Hirata, CERN Report NO. 88-04, (2016)

Construction of the basic control system with VEE for developing a fiber laser oscillator

Sousei Inada[a,b], Shunya Matsuba[b], and Keigo Kawase[b]

[a]*Department of Physical Science, Faculty of Science, Hiroshima University*
1-3-1 Kagamiyama, Higashi Hiroshima, Hiroshima 739-8526, Japan
[b]*Hiroshima Synchrotron Radiation Center, Hiroshima University*
2-313 Kagamiyama, Higashi Hiroshima, Hiroshima 739-0046, Japan

Keywords: fiber laser, control system

Ultrashort pulses generated by a mode-locked laser system are widely used in various scientific and industrial fields. A fiber laser system is a remarkable tool to generate ultrashort laser pulses because of its compactness, stability, and ease of handling. At the field of accelerator science, the short-pulse laser system is well used for various purposes, thus, our group will start the development of ultrashort pulse laser system using Ytterbium doped fiber.

At the development of laser system, it is also important to develop peripheral technologies. In this study, especially we make the basic system to control and monitor the frequency and laser power measuring devices using programming environmental software VEE by Keysight Technologies. In this presentation, we will show the summary of the basic control system which we constructed and examples of the measurement results for the characteristics of the long-term stability for an arbitrary waveform generator and frequency counter and for the output power of fiber laser in dc-operation mode.

Research Activities

– Instrumental Developments –

Current status of Rotatable high-resolution ARPES system at the linear Undulator Beamline at HiSOR

E. F. Schwier[a], H. Iwasawa[b], Y. Aiura[c], K. Shimada[a]

[a]*Hiroshima Synchrotron Radiation Center, Hiroshima University, Higashi-Hiroshima, Hiroshima 739-0046, Japan*
[b]*Diamond Light Source, Harwell Campus, Didcot OX11 0DE, Oxfordshire, United Kingdom*
[c]*National Institute of Advanced Industrial Science and Technology, Tsukuba, Ibaraki 305-8568, Japan*

Keywords: angle resolved photoelectron spectroscopy

The end-station at the linear undulator beamline at HiSOR (BL-1) has been upgraded, focusing on the flux for higher energy photons (I), usability of the beamline optics (II) and sample preparation capabilities (III). The overall performance and capabilities of the beamline have been recently described in [1].

I. High photon energy performance

Extensive optimization of the optical elements within the beamline has been performed. This leads to an increase of photon flux for energies above 100 eV. The increased flux allows for an extension of ARPES measurements beyond 100 eV, while retaining useful energy resolutions and measurement time scales. As an example, Figs. 1(a) and 1(b) respectively show the Fermi surface mappings of Fe(001) thin films taken at hν = 155 eV (bulk H-point of Fe) in the *p*- and *s*-polarization geometries. The acquisition time of the measurements was ~ 40 min. At these photon energies, the cross-section for surface derived states is greatly reduced. This gives access to the bulk energy dispersion within the band structure. In the case of Fe(001), if measured at photon energies below 100 eV, essentially all of the spectral weight at the Fermi level is surface derived with only very weak bulk contributions [2]. At high enough photon energies, however, the band structure seems to be dominated by bulk derived states, as evidenced by the significant difference between the Fermi surface taken at hν = 155 eV and 145 eV in the *s*-polarization geometry (Figs. 1(b) and 1(c)).

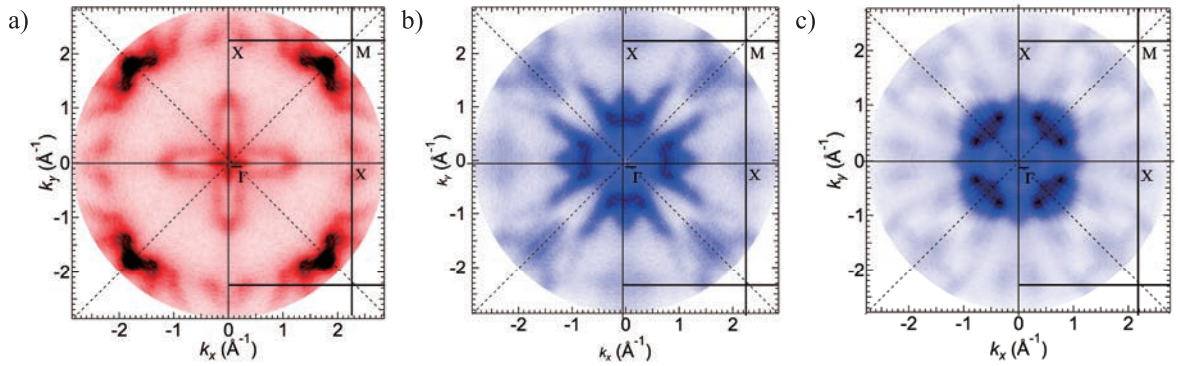

FIGURE 1. Fermi surface of Fe(001) thin film grown on MgO(001) taken at hν = 155 eV (bulk H-point) at 10 K in (a) the *p*-polarization geometry and (b) the *s*-polarization geometry. (c) Fermi surface taken at hν = 145 eV (off H-point) taken in the *s*-polarization geometry demonstrating the bulk-like dispersion of the majority of the Fermi surface features.

II. Usability of beamline optics

A newly developed LabVIEW software has been installed in order to drive the beamline optical elements during changes of the photon energy. The software calculates optimal positions and drives motors of the main optics elements (GR pitch, S2 Move) in a parallel-automated way, thus decreasing the overall time of each photon energy change. It also allows a fine-tuning of the photon flux in a manual mode (M1 pitch, GR pitch) and calculates the undulator gap settings. The overall reduction of the time per photon-energy change greatly increased the incentive for users to perform photon energy dependent measurements of the bulk dispersion, i.e.

k_z mappings. As an example Figure 2 shows the band dispersion of Ni(001) along the ΓX direction in *s*-polarization geometry around the bulk X-point acquired over 2 h. [3] Strong matrix element effects can be seen to be present at any given photon energy, leading to strong asymmetries in the spectral weight at any given photon energy. Only the complete k_z map allows a precise determination of the photon energy corresponding to the X-point in Nickel.

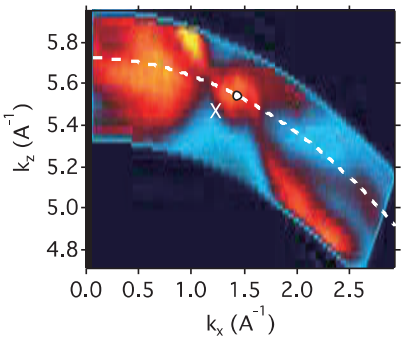

FIGURE 2. Bulk band dispersion of the electronic band structure of Ni(001) around the bulk X-point as a function of k_z and $k_{||}$ along the GX direction. The photon energy range was 100 eV – 125 eV in steps of 1 eV. The X-point was determined to be located at hν = 115 eV.

III. Sample preparation

In order to improve the sample preparation capabilities at the end-station, we installed a new high temperature annealing system in the preparation chamber, as well as an in-situ deposition system in the main chamber.

The high temperature annealing system allows for annealing temperatures of ~ 2000°C and even higher flash temperatures, while retaining UHV conditions. Sample annealing in O_2 atmosphere or surface treatment via H_2 cracker were also installed and tested on various surfaces.

The in-situ deposition system in the main chamber allows for the deposition of metals (e.g., Na, K, Au) on the sample surface in coincidence with the ARPES measurement, while keeping vacuum pressures ~1×10^{-8} Pa. Measuring ARPES in coincidence during the deposition leads to three main advantages of the current system over classical in-situ deposition: (1) It is possible to carefully monitor the deposition with a high time sampling rate, thereby resolving possible kinks in the deposition dependent evolution of core-levels or surface states [4]. (2) It allows for a fine tuning of the doping level to the desired degree of surface modification, e.g. emergence of a surface state. (3) The generally larger distance of the deposition source reduces the influence of thermal heating to the sample surface, allowing true surface doping without induced surface mobility of adatoms.

Here we show the first proof-of-concept measurements performed by deposition of Au on the topological insulator Bi_2Se_3 [5]. In Figure 3, the spectral weight at the Fermi level along the ΓM direction is plotted as a function of time. Before the deposition, the Dirac cone has a k_F of 1°. Once the deposition starts at t=7 a linear increase of band filling of the Dirac cone can be easily observed. Around t=72 the 2 dimensional surface electron gas (2DEG) emerges visibly at k_F ~ -1.1°. Even though the deposition rate was constant (as evidenced by measurements of the Au 5d core-level) the change of the doping is almost zero until at t=130 the deposition is stopped and no more change occurs.

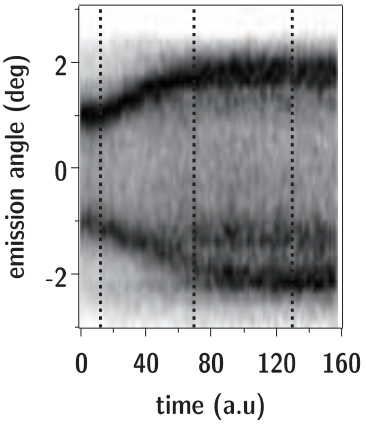

FIGURE 3. Example of time evolution of the k_F of the Dirac cone as a function of time during Au deposition on Bi_2Se_3 at hν=50 eV and T=20 K. Deposition starts at t=7 and stops at t=130 marked by dotted lines. The emergence of the 2DEG around t=72 is also marked by a dotted line.

References

1. H. Iwasawa, K. Shimada, E. F. Schwier et al., J. Synchrotron Rad. (2017) in press
2. K Shimada et al., HiSOR proposal number 16AG038
3. E. F. Schwier et al., HiSOR proposal number 16AG034
4. E. F. Schwier et al. HiSOR proposal number 14AG041
5. E. F. Schwier et al. HiSOR proposal number 16AG035

Current Status of VUV-laser-based μ-ARPES at HiSOR

E. F. Schwier[a], H. Iwasawa[b], M. Arita[a], A. Ino[a], Y. Aiura[c], K. Shimada[a], H. Namatame[a], M. Taniguchi[a]

[a]*Hiroshima Synchrotron Radiation Center, Hiroshima University, Higashi-Hiroshima, Hiroshima 739-0046, Japan*
[b]*Diamond Light Source, Harwell Campus, Didcot OX11 0DE, Oxfordshire, United Kingdom*
[c]*National Institute of Advanced Industrial Science and Technology, Tsukuba, Ibaraki 305-8568, Japan*

Keywords: scanning ARPES microcopy, self-energy analysis, Laser-based ARPES

Strongly correlated materials exhibit various intriguing and drastic phenomena such as metal-insulator transitions, high-Tc superconductivity and colossal/giant magnetoresistance. When multiple phases are adjacent and competing in the vicinity of the first-order phase transition for instance, self-organized electronic inhomogeneity with various types and length scales emerges [1]. In order to find deeper insight into the macroscopic phenomena in these materials, it is indispensable to understand local electronic structures with relevant spatial resolution. High-resolution ARPES has been a prime tool to investigate them. However, if spatial inhomogeneity (by phase separation or surface quality) is combined with low energy scales of the relevant excitations, the demands on the lateral resolution of ARPES increase while high energy and angular resolution is still needed. To remedy this problem we continued to improve our *μ-ARPES* system [2] by combining the advantages of conventional high-resolution laser ARPES and spatially-resolved scanning PES; we installed an XYZ stage with sub-μm precision of movement as well as an optical lens system to focus our laser beam down to ~5 μm. To achieve sub meV energy resolution, the pulse width was set to be ~10 ps, and the repetition rate was chosen to be 80 MHz to avoid space-charge effects. Freely adjustable light polarization provided by waveplates increases the versatility of our system [3] and allow us to investigate the electronic structure of a wide range of materials with very high quality. The machine setup is described in detail in [4]. Our *μ-ARPES* machine is able to reveal both intrinsic and extrinsic spatial inhomogeneity in the electronic structure with outstanding accuracy [5].

In Fig. 1(a) we show a scanning photoemission microscopy (SPEM) measurement performed on a $Bi_2Sr_2CaCu_2O_{8+\delta}$ sample by integrating the total ARPES intensity around the nodal line. The SPEM is well comparable to the high-resolution optical image (Fig. 1(b)) obtained ex-situ after the measurement. Flat areas of the surface with homogeneous intensity can be easily identified.

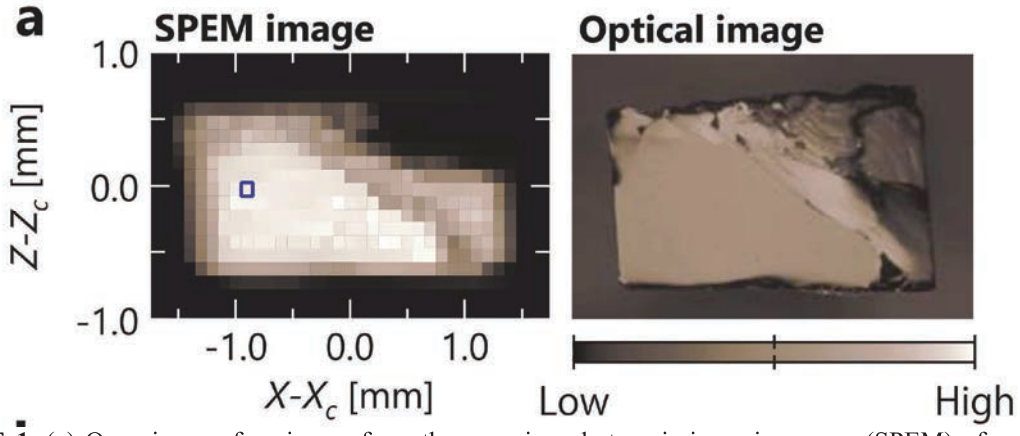

FIGURE 1. (a) Overview surface image from the scanning photoemission microscope (SPEM) of overdoped $Bi_2Sr_2CaCu_2O_{8+\delta}$ (T_c=75 K) taken with 6.36 eV at 12.5 K. Typical raw scanning μ-ARPES data with an acquisition time of 5 sec along the nodal direction. (b) Optical microscope image of the sample measured ex-situ after the SPEM measurement.

The small rectangle at (X-X_c, Z-Z_c) = (-1.0, 0.0) in Fig. 1(a) was chosen for further investigation. A detailed SPEM map was acquired over an area of 100 x 100 μm^2 with a step size of 5 μm. Figure 2 shows the results of a quantitative analysis of the nodal band.

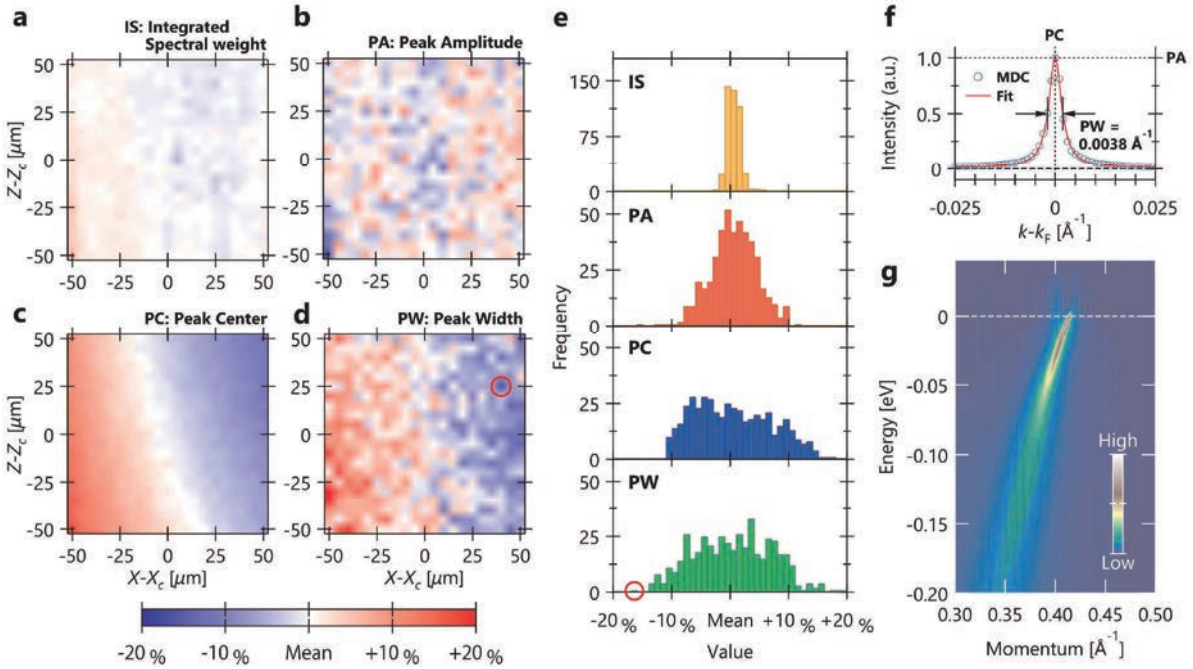

FIGURE 2. High-resolution and fine scanning μ-ARPES results from overdoped $Bi_2Sr_2CaCu_2O_{8+\delta}$ (T_c=75 K) taken with 6.36 eV at 12.5 K. (a) Expanded SPEM image measured at the 100×100 μm^2 region indicated by the square in Fig. 1(a). (b)-(d) Spatial evolution of the results of spectral lineshape analysis on ADCs at E_F±10 meV: (b) peak amplitude, (c) peak center, and (d) peak width. All the values shown in (b)-(d) are rescaled by the mean value across the whole measurement region. (e) Histograms of (a)-(d) from the top to bottom. (f) MDC at E_F sliced from (g) together with the function fit (red line). (g) High-statics nodal ARPES image taken at the micro-spot indicated by the circle in (d) and (e).

While the total integrated spectral weight spatial map (Fig. 2(a)) does not show significant variation across the 100x100 μm^2 region, one can recognize more inhomogeneity in the images which represent the spatial distribution of the peak amplitude (Fig. 2(b)), peak center (Fig. 2(c)) and the FWHM (of the Lorentzian function obtained by fitting ADCs at E_F±10 meV. Especially the latter two values show significant fluctuations of about ±20% against the mean value on length scales accessible to our μ-ARPES machine. Using a Histogram plot of the fitting parameters (Fig. 2(e)) one can easily deduce the Gaussian-like distribution of peak intensity and height, while the emission angle and the FWHM exhibit a more complex distribution across the measurement region. More important for the extraction of intrinsic quantities is the fact that the lateral resolution in the variation of the FWHM allows one to choose optimized measurement positions to improve the measurement of self-energy and band dispersion in general. In the case of $Bi_2Sr_2CaCu_2O_{8+\delta}$ (T_c=75 K) a FWHM of 0.0038 Å^{-1} could be extracted (Figs. 2(f) and 2(h)) which is the smallest line width for this material reported so far. The choice of the measurement position clearly allows one to reduce the effects of intrinsic surface/bulk defect broadening. The small spot-size of the photons, on the other hand, leads to a reduction of the overall angular resolution broadening of the analyzer. Fitting the ADC in Fig. 2(f) with a Voigt function we could extract the Gaussian and Lorentzian contribution to the FWHM. The Gaussian width corresponds to an angular broadening of ~ 0.05° which contributes only 2% to the total width of the peak.

We are currently implementing a software that allows to keep the measurement position constant with respect to the light and analyzer axes, while allowing for rotations of the DPRF and tilt angles. Especially the latter is important to map the electronic structure of the Fermi surface.

References

1. Nanoscale Phase Separation and Colossal Magnetoresistance, edited by E. Dagotto (Springer, 2002).
2. H. Iwasawa & E. F. Schwier et al., Activity report 2015
3. W. Mansur & K. Tokura *et al.*, HiSOR symposium poster P24S, 2017.
4. H. Iwasawa & E. F. Schwier et al., Ultramicroscopy submitted 2017
5. M. Watson *et al.*, J. Phys. Soc. Jpn. **86**, 053703 (2017).